Potassium ions in the cavity of a KcsA channel model

Zhenwei Yao, Baofu Qiao, and Monica Olvera de la Cruz
Department of Materials Science and Engineering, Northwestern University, Evanston, Illinois 60208-3108, USA
(Received 26 July 2013; revised manuscript received 23 October 2013; published 13 December 2013)

The high rate of ion flux and selectivity of potassium channels has been attributed to the conformation and dynamics of the ions in the filter which connects the channel cavity and the extracellular environment. The cavity serves as the reservoir for potassium ions diffusing from the intracellular medium. The cavity is believed to decrease the dielectric barrier for the ions to enter the filter. We study here the equilibrium and dynamic properties of potassium ions entering the water-filled cavity of a KcsA channel model. Atomistic molecular dynamics simulations that are supplemented by electrostatic calculations reveal the important role of water molecules and the partially charged protein helices at the bottom of the cavity in overcoming the energy barrier and stabilizing the potassium ion in the cavity. We further show that the average time for a potassium ion to enter the cavity is much shorter than the conduction rate of a potassium passing through the filter, and this time duration is insensitive over a wide range of the membrane potential. The conclusions drawn from the study of the channel model are applicable in generalized contexts, including the entry of ions in artificial ion channels and other confined geometries.

DOI: 10.1103/PhysRevE.88.062712 PACS number(s): 87.16.Vy, 87.10.Tf, 87.15.A−, 87.17.Uv

I. INTRODUCTION

Ion transportation through pores in membranes is a crucial process in cell biology [1]. The regulation of ion passage is realized by ion channels, the fundamental excitable elements in the membranes of excitable cells [2]. Specifically, potassium ion channels represent an important class of ion channels, and they are responsible for maintaining a membrane voltage gradient of excitable cells to realize various biological functions, such as driving the production of Adenosine triphosphate in mitochondria and transmitting electric signals [2,3]. The most striking properties of potassium ion channels include the high rate of ion flux at the order of 10^7–10^8 ions per second approaching the theoretical limit of unrestricted diffusion and the remarkable selectivity for potassium ions to pass about 1000 times more readily than for sodium ions [3]. One key question about potassium ion channels is how they are able to achieve such a fast throughput rate while maintaining strong selectivity for potassium over sodium ions [4,5]. An understanding of this question facilitates the design of smart nanoscaled artificial channels that can ultimately lead to the development of molecular and nanosensing devices [1,6–8].

The progress in the structural characterization of KcsA channel from *Streptomyces lividans* provides us the opportunity to understand this open question [9,10]. Extensive theoretical work follows, including the continuum electrostatic model [11,12], the Brownian dynamics simulations [13], and Poisson-Nernst-Planck calculations [14]. A KcsA potassium ion channel consists of a water-filled cavity and a filter that is made of four identical twisted subunits spanning the membrane, with the wide end of the channel facing the extracellular space, as shown in Fig. 1. The fast throughput rate has been attributed to several factors, including the repulsion between potassium ions in the selectivity filter [9,15], the energetic balance of two possible ion configurations [16,17] and the ion-dependent conformational change within the selectivity filter [18].

All the above explanations for the fast ion flux rate in potassium ion channels are related to the ions in the filter. A filter connects the channel cavity and the extracellular environment; the potassium ions in the cavity serve as the reservoir. It seems that there are sufficient potassium ions inside the cell, where its concentration is greater than 100 mM [10]. Potassium ions keep diffusing to the cavity from the intracellular side as the ions already in the filter are pushed to the extracellular side. It is natural to ask if the flux rate of ions entering the cavity can catch the speed of outflux at the extracellular side of the selectivity filter. A very recent atomistic simulation shows that trapped ions in the cavity will wait for a few microseconds before permeating through the filter to the extracellular side for the voltage-gated potassium ion channels Kv1.2-2.1 in some range of membrane potential, indicating that the influx rate of ions to the cavity is faster than the outflux rate to the extracellular side for these specific potassium ions [19]. A general understanding to this problem without considering the atomic details of the channel structure is of biomimetic significance for the design of artificial channels. To address this problem, we study the equilibrium and dynamic properties of potassium ions confined in the water-filled cavity of an open KcsA channel model using atomistic molecular dynamics (MD) simulation method complemented by arguments based on electrostatics.

The process of an ion entering the cavity of a potassium ion channel is highly involved; several factors are delicately influencing the whole process, including the ion concentration, the hydration of ions, the charge distribution in membrane proteins, and the voltage-sensing domain [19]. However, extensive studies have shown that various features of ion channels have an electrostatic origin. Specifically, the permeation, selectivity, and gating of ion channels can be largely understood by electrostatics [20]. In light of the significance of electrostatics in ion channel systems, we first resort to a pure electrostatic calculation about the energetics of a single K^+ ion in the cavity of a KcsA channel to understand the entry of ions to the cavity. Our calculations based on a simplified KcsA channel model show that the optimal position of the ion is at the center of the channel, and the energy minimum is relatively broad. These features are consistent with a more detailed and thus

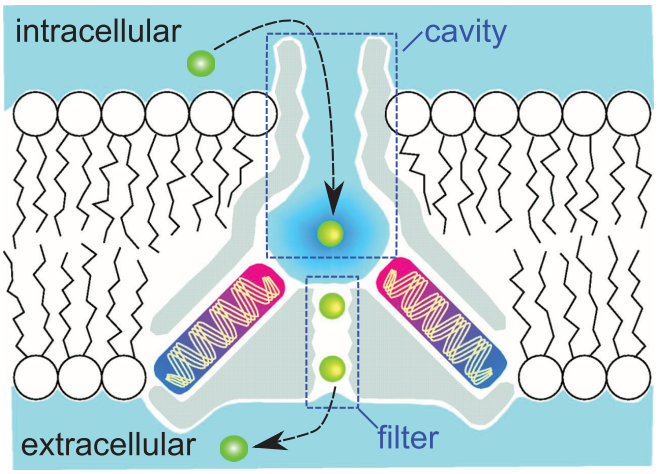

FIG. 1. (Color online) Schematic plot of a KcsA channel in a cell membrane. A potassium ion is stabilized in the water-filled cavity partly due to the oriented helices pointing their partial negative charge (carboxyl end, red) towards the cavity. The picture is excerpted from Ref. [9] with modifications. Reprinted with permission from AAAS.

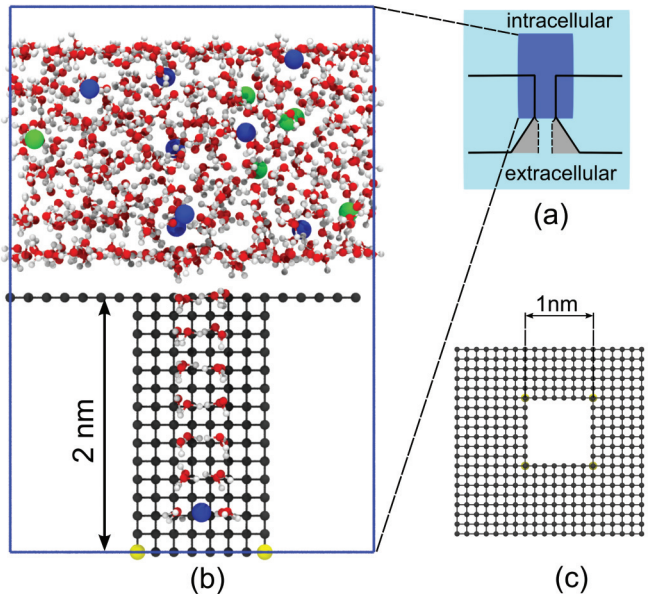

FIG. 2. (Color online) (a) Schematic representation of the location of our simulation box (the left larger blue box) in the KcsA channel. (b) Side view of the simulation box in the last frame of a simulation, where K^+ and Cl^- are highlighted in blue and green, respectively. The cavity is composed of two parts: the negatively charged bead ($-0.75|e|$ per bead) in yellow and the gray wall beads to mimic the cavity wall. Some cavity beads are removed for the display of the waters and the K^+ distributed inside the cavity. (c) Top view of the cavity.

more expensive calculation, where the channel is represented in full atomic detail with all explicit partial charges [19,21]. This consistency implies the effectiveness of pure electrostatic analysis, despite the biological complexity of the system. In addition, by comparison with the results from atomistic MD simulations, we identify the crucial role played by both the partially charged protein helices at the bottom of the cavity and the water molecules in the cavity in reducing the entry barrier of ions and their stabilization in the water-filled cavity. Finally, we show that the average time τ for a potassium ion to enter the cavity is much shorter than the conduction rate of a potassium ion passing through the filter, and the value of τ is insensitive over a wide range of the membrane potential.

II. ATOMISTIC MD SIMULATION METHODOLOGY

Considering its fourfold rotational symmetry, we model the cavity shape of a KcsA channel as a square cylinder (see Fig. 2). The side length of the square cross section is 1 nm and its length is 2 nm for the cavity. This oversimplified shape captures the length scale and the symmetry of the KcsA channel and can be generalized to other ion channels at the price of sacrificing the molecular details of the KcsA channel. Four negative charges q are placed at the bottom of the cavity, mimicking the four partially charged helices in the KcsA channel [21]. We set $q_a = -0.75|e|$ (or $-|e|$). The simulation box is first filled with about 500 water molecules. Then 9 water molecules are replaced with 9 K^+ ions and another 6 water molecules with 6 Cl^- ions, all located outside the cavity. Therefore, the system is charge neutral. The concentration of K^+ ions is around 1 mol/L.

Classical MD simulations are performed using the package GROMACS (version 4.5.5) [22]. The atomistic OPLS-AA force field [23] is employed, in combination with the SPC/E water model [24] whose geometry is constrained using the SETTLE algorithm [25]. Note that in the atomistic MD simulation where water molecules are treated explicitly, the screening effect associated with water molecules has been included that is distinct from the image charge effect in continuum electrostatics. The length scale of the simulation box is $2.8 \times 2.8 \times 4.2\ \text{nm}^3$ ($X \times Y \times Z$) according to the size of the KcsA channel. The wall of the cavity is composed of two parts, as illustrated in Fig. 2. To depict the hydrophobic interior of cell membranes, the wall beads in gray are introduced, each of which is represented by a neutral hydrocarbon atom possessing Lennard-Jones 12-6 interaction with waters and ions. Charged beads in yellow are utilized to mimic the charged groups on proteins embedded in the KcsA channel. Two implicit wall potentials in Lennard-Jones 10-4 form [22] are introduced at the top and the bottom of the simulation cell to prevent the escape of waters and ions. All the wall beads are kept frozen throughout the simulations.

The energy of the constructed system is first minimized via the steepest descent algorithm. In production runs, the two-dimensional (2D) periodic boundary condition (PBC) is employed in the X-Y plane. The electrostatic interactions are calculated using the smooth particle mesh Edward (PME) method [26,27] with a direct space cutoff of 1.2 nm and a Fourier grid spacing of 0.12 nm. Note that even though the reciprocal summation of the Edward algorithm is performed in 3D, a dipolar correction term [28] is utilized for a pseudo-2D summation. Moreover, a void region of $z_{\text{void}} = 4.2$ nm is introduced in the Z dimension to reduce the artifacts in Edward summation from the unwanted third dimension, which results in the overall length in Z dimension of 8.4 nm. Lennard-Jones interactions and forces are cut at 1.2 nm with the long-range dispersion corrections to the potential energy and the pressure

applied. The MD integration time step of 2 fs is employed with all the covalent bond lengths constrained via the LINCS algorithm [29]. The canonical ensemble (constant number of particles, temperature, and volume, NTV) is employed, with the temperatures of waters and ions being separately scaled via the Nosé-Hoover thermostat (reference temperature 298 K, characteristic time $\tau = 0.5$ ps). Each of the simulations is performed for a duration of 10 ns.

III. RESULTS AND DISCUSSION

The importance of electrostatics in analyzing the behaviors of ion channels in solutions has been extensively reported [21,30,31]. We first resort to a pure electrostatic calculation about the energetics of a single K^+ ion entering the cavity of a KcsA channel. The entry of potassium ions to the cavity is impeded by the high contrast of the dielectric constant of water and that of the lipid membrane; the dielectric constant of a lipid membrane is only 1–2, in contrast to that of water, as high as 80 at room temperature. Consequently, polarized charges are induced in the interface of water and the lipid membrane.

In order to calculate the electrostatic energy associated with the image charge effect, we treat the water-filled cavity as a rigid geometry neglecting the fluctuation in the functionally important regions of the channel structure in the process of an ion entering the cavity, as disclosed in MD simulations of an atomistic model of the KcsA potassium ion channel [32]. According to the fourfold symmetry of the KcsA channel, we model the cavity as a square cylinder whose cross section is a square of side length 1 nm [Fig. 2(c)]. The dielectric constants inside (where the water molecules are treated as a continuum medium) and outside the cavity (lipids and proteins) are ϵ_1 and ϵ_2, respectively. Although it is inappropriate to treat water molecules in a nanoscaled confined geometry as a continuum dielectric medium due to the increasing importance of interactions between the substrate and water molecules [33–35], the continuum model of water molecules is of value in providing conceptual understanding of the system and serves as a complementary tool for more detailed atomistic MD simulations, as explained below. Specifically, the comparison of the continuum model for water and atomistic MD simulations in this work can reveal the particular role of the microscopic structure of water molecules in stabilizing ions in the cavity.

For a K^+ ion inside the square cylinder, we consider the four induced image charges corresponding to each plane and the eight secondary image charges while neglecting the higher order image charge effect that is compatible with the precision of the model. Since the radius of the K^+ is much smaller than the length of the cavity, we treat the plane as infinitely large and the ion as a point charge. The profile of the energy barrier for an ion entering a cylindrical channel from its end has been calculated in a continuum electrostatic model; the magnitude of the peak of the energy barrier [11] qualitatively agrees with our calculations, as shown later. The sharp contrast in dielectric constants and the length scales are captured despite the simplicity of the model. Now consider a point charge q located at the distance a ($x = y = 0, z = a$) away from the planar boundary (X-Y plane) of two dielectric mediums. The point charge is in the medium of dielectric constant ϵ_1, where the electric potential is

$$\psi = \frac{q}{4\pi\epsilon_1}\left[\frac{1}{\sqrt{x^2+y^2+(z-a)^2}} + \frac{\epsilon_1-\epsilon_2}{\epsilon_1+\epsilon_2}\frac{1}{\sqrt{x^2+y^2+(z+a)^2}}\right]. \quad (1)$$

The second term denoted as V_{img} originates from the image charge $q' = (\frac{\epsilon_1-\epsilon_2}{\epsilon_1+\epsilon_2})q$ [36]. For $\epsilon_1 > \epsilon_2$, the image charge and the original one have the same sign, so a potassium ion in the cavity is repelled by its image charges. The potential energy of the charge q is $W = \frac{1}{2}qV_{\text{img}}$. We carry out the same calculation for the four walls of the cavity. Note that the limited amount of water molecules in the cavity may reduce their dielectricity in comparison with bulk water [34]. An effective dielectric constant of confined water molecules surrounding an ion may be introduced. $\epsilon_{\text{eff}} \approx 25$ according to the energy barrier of 6.3 kcal/mol for the transfer of a single potassium ion from the intracellular side to the cavity based on molecular simulations in full atomic detail including the irregular shape of proteins [21]. ϵ_{eff} is modestly underestimated due to the neglect of the higher order image charges that reduces the magnitude of the energy barrier. The result that $\epsilon_{\text{eff}} < \epsilon_{\text{water}} \approx 80$ indicates a diminished screening capability of the limited amount of water molecules inside the channel.

Figure 3 shows the energy of the system due to the image charge effect as the ion transversely moves by Δx from the center of the squared cross section of the channel. We see that the sharp contrast in dielectric constants lowers the energy for an ion to enter the channel from about $18k_BT$ to $4k_BT$ as ϵ_1 increases from 5 to 80. The basic shape of the energy profiles in Fig. 3 is insensitive to the variation of the dielectric constant. It is important to note the broad energy minimum and the abrupt increase of the energy near the wall. The ion is therefore confined in the flat region of the energy profile due to the strong repulsion near the wall; the polarized charges on the channel wall effectively shrink the transversal size of

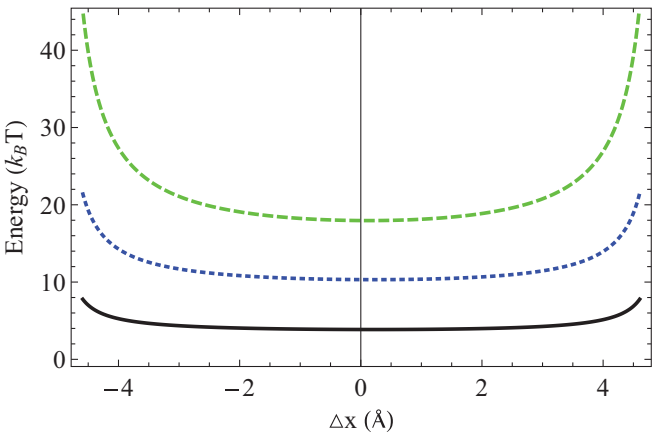

FIG. 3. (Color online) The energy of a point charge that is deviated by Δx from the center of a square along the direction parallel to its side. The length of the square is 1 nm, which is the size of the cavity of KcsA potassium ion channel. The dielectric constants inside the cavity are $\epsilon_1 = 80$ (solid black line), 25 (dotted blue line), and 5 (dashed green line). $\epsilon_2 = 2$ outside the cavity.

the channel in addition to elevating the energy level. These features enable one to ignore the image charge effect in some situations as an approximation, such as the determination of the equilibrium locations of ions in the cavity that are discussed later. This energy landscape of the interaction of the ion and its images is consistent with a more detailed calculation of the electrostatic energy of the system where the channel is represented in full atomic detail with all explicit partial charges [21]. This consistency implies the significance of the sharp dielectric constant, which has been highlighted in our model, in characterizing the basis features of the ion channel system. Note that the profile of a flat energy landscape surrounded by steep walls is also found in the conducting cubic cavity [37].

Our calculation shows that thermal fluctuations ($\approx k_B T$) at room temperature fail to conquer the energy barrier for a potassium ion to enter the cavity for $\epsilon_1 = \epsilon_{\text{eff}} \approx 25$. An extra driving force is therefore required to pull potassium ions to the cavity. Structural characterization has revealed that the four oriented pore helices at the bottom of the cavity may be the structural basis for overcoming the dielectric barrier [9], which we discuss later. On the other hand, the featured flat energy landscape in a broad range of the value for ϵ indicates that thermal fluctuations at room temperature can drive a potassium ion away from the center of the channel until very close to the wall. However, a potassium ion sitting at the center of the cavity has been observed at 2.0 Å resolution in Ref. [10]; it is suggested that the hydration shell around the K^+ ion that is connected to the wall of the cavity is responsible for the observation.

To understand the influence of water molecules on the equilibrium position of potassium ions in the KcsA cavity, we perform atomistic MD simulations where water molecules are explicitly represented by the SPC/E water model [24] that can capture its more detailed information than a continuum electrostatic model and thus provides new insights into the system. For example, simulations of a number of channel models have shown substantially different dynamic properties of water molecules in a cylindrical pore from those in the bulk [38]; in particular, the translational and rotational mobilities are reduced, and the confined water molecules display a higher degree of order than in bulk [39–41]. A series of atomistic MD simulations capture the event of two potassium ions entering the cavity due to the attraction of the negatively charged helices at the cavity bottom. The trapped potassium ions are found to be aligned along the symmetry axis of the channel in most cases; their equilibrium positions are plotted in Fig. 4 for 20 independent simulations. The negative charge on each of the four helices is set to be $q_a = -|e|$. We do not consider the membrane potential to highlight the effect of water molecules on the equilibrium positions of potassium ions. The average positions of the two ions locate at $\bar{z_1} = 0.28$ nm (read from the blue bars in Fig. 4) and $\bar{z_2} = 0.62$ nm (from the red bars), respectively.

Now we compare these simulation results with electrostatic calculations. With the position of the first ion near the cavity bottom fixed and without considering the image charge effect, the equilibrium position of the second ion can be obtained by minimizing the electrostatic energy,

$$E(\vec{r}_K) = \frac{q^2}{4\pi\epsilon_w}\left(\sum_{i=1}^{4}\frac{-1}{|\vec{r}_i - \vec{r}_K|} + \frac{1}{|\vec{r}_{\text{ion}} - \vec{r}_K|}\right), \qquad (2)$$

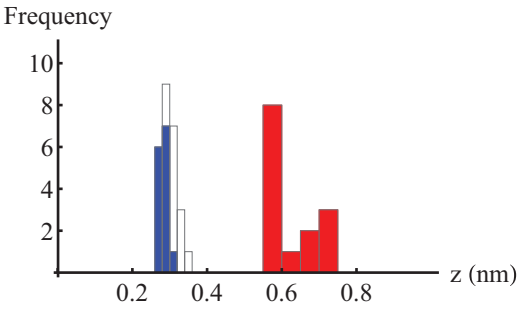

FIG. 4. (Color online) The distribution of the equilibrium positions of a single trapped potassium ion ($q_a = -3|e|/4$, white open bars) and the two ions [$q_a = -|e|$, blue (left) and red (right) bars] in the cavity obtained by independent simulations. There is some overlap between the white and the blue (left) bars. The four charged helices lie in the $z = 0$ plane.

where $\vec{r}_i$ is the position of the four α helices and $\vec{r}_{\text{ion}}$ is the position of the first potassium ion already in the cavity. $\vec{r}_K$ is the position of the second potassium ion whose equilibrium value is to be determined. We notice in the expression for $E(\vec{r}_K)$ that the optimal value for $\vec{r}_K$ is independent of the dielectric constant of water. In other words, for the second potassium ion, due to the weakened dielectric ability of water the enhanced attraction from the negatively charged α helices and the enhanced repulsion from the first potassium ion are canceled out that the determination of its equilibrium position is finally independent of the specific value of the dielectric constant of water. With $z_1 = \bar{z_1} = 0.28$ nm, we have $z_2 = 0.92$ nm $> \bar{z_2}$. By considering the image charges of the first cation which are also positively charged, the second potassium ion will be pushed further away from the cavity bottom. It indicates that the existence of water molecules (in atomistic MD simulations) significantly reduces the distance between the two trapped potassium ions. The water molecules do screen the Coulomb repulsions between these two ions; this screening effect, however, is not captured by the continuum model of water molecules.

In atomistic MD simulations, a potassium ion inside the cavity is found to be on the axis of the channel in most runs. Pure electrostatic analysis, however, shows a distinct picture. Here we calculate the electrostatic interaction energy of the potassium ion and the four negative charges at the bottom of the cavity, based on which we search for the equilibrium location of the ion. Considering that the image charges have weak influence on the equilibrium location of the ion as shown in Fig. 3, the interaction of the ion with the four negative structural charges is neglected in our calculation. Figure 5 shows the energy landscape of a K^+ ion in the cavity over the planes perpendicular to the channel axis at various heights; the larger the value of z is, the further away the ion is from the bottom of the cavity. The optimal position of the K^+ ion moves from the axis to the corner of the channel with the decrease of the distance [from Figs. 5(a) to 5(d)]. Considering the smallness of a potassium ion whose ionic radius is only 0.138 nm, potassium ions can get access to the regions of these four corners corresponding to the energy minima as shown in Fig. 5(d). In addition, electrostatic calculations show that in

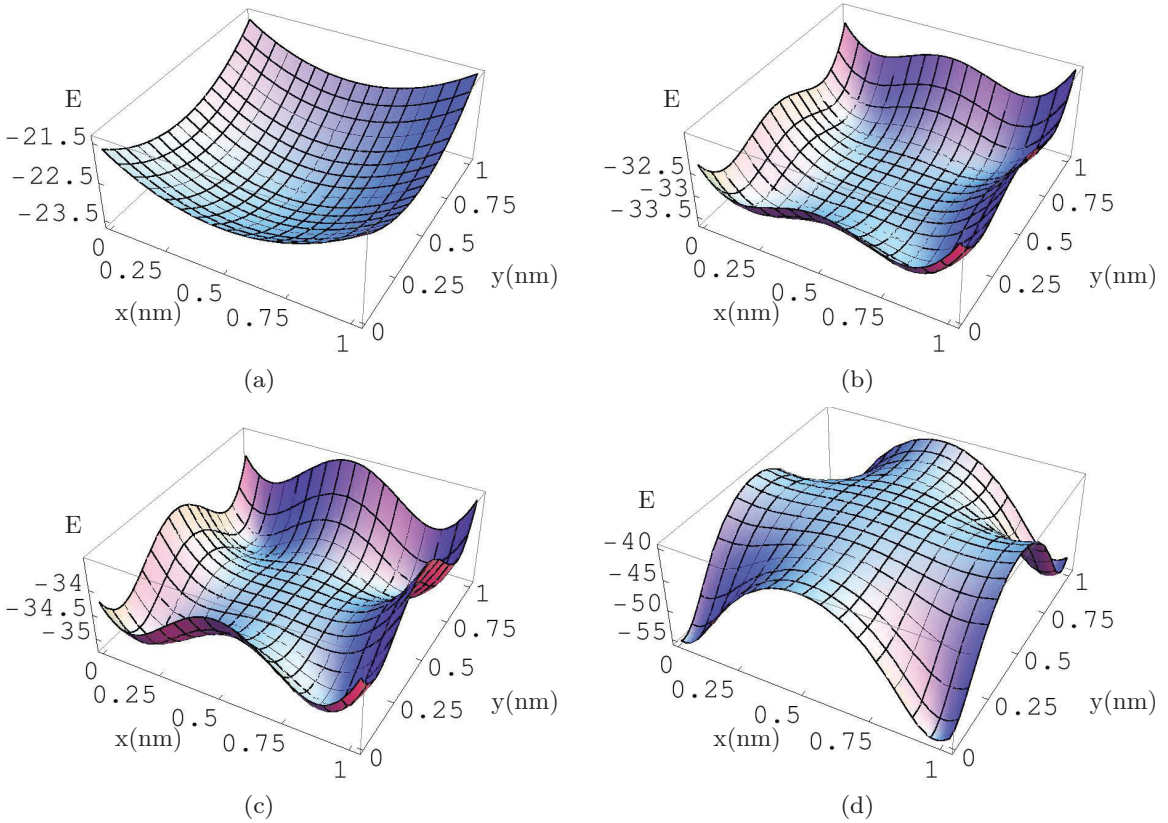

FIG. 5. (Color online) The energy landscape of a K^+ ion in the cavity over the planes perpendicular to the channel axis at various heights exclusively due to the charged pore helices; $z = 1.0$ nm (a), 0.5 nm (b), 0.45 nm (c), and 0.2 nm (d). The energy is measured in units of $k_B T$.

the energy landscape at the height $z = 0.45$ nm [see Fig. 5(c)] four energy minima have already been obviously developed. It indicates that the finite size of the cation does not prevent its collapse to one of the charged helices. In atomistic MD simulations, largely due to the existence of water molecules between the K^+ ion and the charged helices, the collapse of the K^+ ion to one of the four fixed negatively charged helices is rarely seen.

In addition to the high dielectricity environment of the water-filled cavity, the polarized negative charges on the pore helices whose COOH terminus are directed towards the cavity (as shown in Fig. 1) facilitate the attraction of potassium ions to the ion channel. The atomistic MD simulations indicate that the amount of the charge q_a on each pore helix can significantly influence the number of potassium ions in the cavity. Figure 4 shows that as $|q_a|$ increases from $3|e|/4$ to $|e|$, an extra potassium ion can be attracted to the cavity. The inclusion of the second potassium ion slightly squeezes the original one towards the cavity bottom ($z = 0$ plane) due to their mutual repulsion. Systematic studies in Ref. [11,12] show that a richer potential energy landscape can be created inside the channel by varying the sites of charged protein residues and the relevant ion dynamics can be subsequently changed. In the design of artificial ion channels, charged elements on the channel wall can therefore be introduced as an essential component to enhance the efficiency of ion flux.

We proceed to study if the flux rate of ions entering the cavity can catch the rate of passing through the filter. Figure 6 shows the entry time for a potassium ion diffusing into the cavity at different electric fields along the Z dimension that are corresponding to different membrane potentials, where the time of entry refers to the time of a potassium ion diffusing to the cavity. In a number of independent simulations, different random seeds are employed in the beginning of the simulations. The average time for a potassium ion to enter the cavity is $\tau = 0.43 \pm 0.39$ ns ($E = 0$ mV/nm), 0.31 ± 0.27 ns (-80 mV/nm), and 0.27 ± 0.16 ns (80 mV/nm), respectively. These time durations are much shorter than the conduction rate of a potassium ion passing through the filter (10–100 ns per ion), indicating that potassium ions diffuse to the cavity much quicker by one or two orders of magnitude than they are pushed out to the extracellular side from the filter. Therefore, the bottleneck of increasing the ion flux lies in the filter. Our

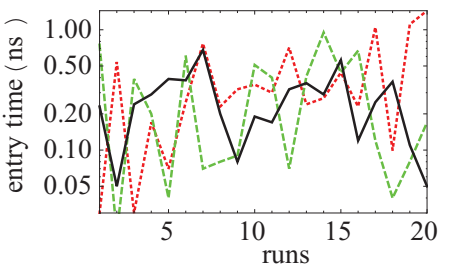

FIG. 6. (Color online) The entry time for a potassium ion diffusing into the cavity at the electric field $E = -80$ mV/nm (dashed green), 0 (dotted red), and 80 mV/nm (solid black) for 20 independent simulations. $q_a = -3|e|/4$.

finding is quantitatively consistent with a simulation work [42], where the passage rate across the channel cavity ($\geqslant$1 ion per ns) was observed to be much faster than the throughput rate (0.02–1 ion per ns) in a Kv 1.2 potassium ion channel. The value of τ seems insensitive to the value of the electric field at least within the range of $E \in [-80,80]$ mV/nm.

Our simulations confirm that the entry of ions to the cavity does not constitute the bottleneck for the fast throughput rate in potassium ion channels, and the principle factor impeding the permeation of ions through potassium ions can be attributed to the selectivity filter. It is important to note that this conclusion is based on the model without any atomic details using much less computational resources. It is therefore of more generality than conclusions based on full atomistic simulations which usually address specific channels.

IV. CONCLUSION

Atomistic MD simulations supplemented by electrostatic calculations reveal the major role played by water molecules and the partially charged protein helices at the cavity bottom among various complicated protein structures of the channel in overcoming the energy barrier and stabilizing the potassium ion in the cavity. We further show that the flux rate of ions entering the cavity can catch the speed of outflux at the extracellular side of the selectivity filter; this flux rate is insensitive over a wide range of the membrane potentials. Our study is based on a simplified KcsA channel model whose basic geometric feature and dielectric contrast are highlighted, while specific atomic details are neglected. Therefore, the conclusions are applicable in generalized contexts, including the entry of ions in artificial ion channels and other confined geometries.

ACKNOWLEDGMENT

We thank the support of the Office of the Secretary of Defense under NSSEFF Program Award No. FA9550-10-1-0167.

[1] C. Maffeo, S. Bhattacharya, J. Yoo, D. Wells, and A. Aksimentiev, Chem. Rev. **112**, 6250 (2012).
[2] B. Hille, *Ionic Channels of Excitable Membranes*, 2nd ed. (Sinauer, Sunderland, MA, 1984).
[3] A. Lehninger, D. Nelson, and M. Cox, *Lehninger Principles of Biochemistry*, 1st ed. (Freeman, New York, 2005).
[4] B. Roux, Annu. Rev. Biophys. Biomol. Struct. **34**, 153 (2005).
[5] R. MacKinnon, Biosci. Rep. **24**, 75 (2004).
[6] S. Majd, E. C. Yusko, Y. N. Billeh, M. X. Macrae, J. Yang, and M. Mayer, Curr. Opin. Biotechnol. **21**, 439 (2010).
[7] H. Bayley and L. Jayasinghe, Mol. Membr. Biol. **21**, 209 (2004).
[8] S. Matile, A. V. Jentzsch, J. Montenegro, and A. Fin, Chem. Soc. Rev. **40**, 2453 (2011).
[9] D. A. Doyle, J. M. Cabral, R. A. Pfuetzner, A. Kuo, J. M. Gulbis, S. L. Cohen, B. T. Chait, and R. MacKinnon, Science **280**, 69 (1998).
[10] Y. Zhou, J. Morais-Cabral, A. Kaufman, and R. MacKinnon, Nature (London) **414**, 43 (2001).
[11] Y. Levin, Europhys. Lett. **76**, 163 (2006).
[12] J. R. Bordin, A. Diehl, M. C. Barbosa, and Y. Levin, Phys. Rev. E **85**, 031914 (2012).
[13] S.-H. Chung, T. W. Allen, M. Hoyles, and S. Kuyucak, Biophys. J. **77**, 2517 (1999).
[14] S. Furini, F. Zerbetto, and S. Cavalcanti, J. Phys. Chem. B **111**, 13993 (2007).
[15] P. Hess and R. Tsien, *Mechanism of Ion Permeation Through Calcium Channels* (Nature Publishing Group, New York, 1984).
[16] J. Åqvist and V. Luzhkov, Nature (London) **404**, 881 (2000).
[17] J. Morais-Cabral, Y. Zhou, R. MacKinnon *et al.*, Nature (London) **414**, 37 (2001).
[18] Y. Zhou and R. MacKinnon, J. Mol. Biol. **333**, 965 (2003).
[19] M. Ø. Jensen, V. Jogini, M. P. Eastwood, and D. E. Shaw, J. Gen. Physiol. **141**, 619 (2013).
[20] P. Jordan, IEEE Trans. NanoBiosci. **4**, 3 (2005).
[21] B. Roux and R. MacKinnon, Science **285**, 100 (1999).
[22] B. Hess, C. Kutzner, D. van der Spoel, and E. Lindahl, J. Chem. Theory Comput. **4**, 435 (2008).
[23] W. Jorgensen, D. Maxwell, and J. Tirado-Rives, J. Am. Chem. Soc. **118**, 11225 (1996).
[24] H. J. C. Berendsen, J. R. Grigera, and T. P. Straatsma, J. Phys. Chem. **91**, 6269 (1987).
[25] S. Miyamoto and P. A. Kollman, J. Comput. Chem. **13**, 952 (1992).
[26] T. Darden, D. York, and L. Pedersen, J. Chem. Phys. **98**, 10089 (1993).
[27] U. Essmann, L. Perera, M. L. Berkowitz, T. Darden, H. Lee, and L. Pedersen, J. Chem. Phys. **103**, 8577 (1995).
[28] I.-C. Yeh and M. L. Berkowitz, J. Chem. Phys. **111**, 3155 (1999).
[29] B. Hess, H. Bekker, H. J. C. Berendsen, and J. G. E. M. Fraaije, J. Comput. Chem. **18**, 1463 (1997).
[30] P. Jordan, Biophys. J. **39**, 157 (1982).
[31] P. Jordan, Biophys. J. **41**, 189 (1983).
[32] S. Berneche and B. Roux, Biophys. J. **78**, 2900 (2000).
[33] P. Gallo, M. Ricci, and M. Rovere, J. Chem. Phys. **116**, 342 (2002).
[34] N. Giovambattista, C. F. Lopez, P. J. Rossky, and P. G. Debenedetti, Proc. Natl. Acad. Sci. USA **105**, 2274 (2008).
[35] S. Sharma and P. G. Debenedetti, Proc. Natl. Acad. Sci. USA **109**, 4365 (2012).
[36] J. D. Jackson, *Classical Electrodynamics*, 3rd ed. (Wiley, New York, 1998).
[37] H. Wu, D. Sprung, and J. Martorell, Eur. J. Phys. **21**, 413 (2000).
[38] M. Sansom, I. Kerr, J. Breed, and R. Sankararamakrishnan, Biophys. J. **70**, 693 (1996).
[39] S. Chiu, E. Jakobsson, S. Subramaniam, and J. McCammon, Biophys. J. **60**, 273 (1991).
[40] G. Hummer, J. C. Rasaiah, and J. P. Noworyta, Nature (London) **414**, 188 (2001).
[41] R. Allen, S. Melchionna, and J. P. Hansen, Phys. Rev. Lett. **89**, 175502 (2002).
[42] M. Jensen, D. W. Borhani, K. Lindorff-Larsen, P. Maragakis, V. Jogini, M. P. Eastwood, R. O. Dror, and D. E. Shaw, Proc. Natl. Acad. Sci. USA **107**, 5833 (2010).